

# UNCLASSIFIED

AD NUMBER
AD855087
NEW LIMITATION CHANGE
TO Approved for public release, distribution unlimited
FROM Distribution authorized to U.S. Gov't. agencies and their contractors; Administrative/Operational; Dec 1968. Other requests shall be referred to Air Force Rocket Propulsion Lab, Edwards AFB CA.
AUTHORITY
AFRPL ltr dtd 27 oct 1971

THIS PAGE IS UNCLASSIFIED

AD855087

# LIQUID PROPELLANT EXPLOSIVE HAZARDS

Final Report - December 1968

VOLUME 3 - PREDICTION METHODS

STATEMENT OF WORK (SOW) 10739  
This document is subject to export controls and may be  
transmitted to foreign countries or persons in foreign countries may be  
made only with prior approval of the Department of Defense.

PREPARED UNDER CONTRACT AF 04 (611) 10739

FOR

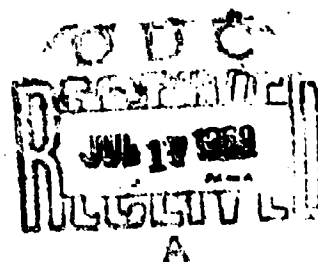
AIR FORCE ROCKET PROPULSION LABORATORY

AIR FORCE SYSTEMS COMMAND

UNITED STATES AIR FORCE

EDWARDS, CALIFORNIA 93523

attn: RPPR-ST/NFO



URS SYSTEMS  
CORPORATION

# LIQUID PROPELLANT EXPLOSIVE HAZARDS

Final Report - December 1968

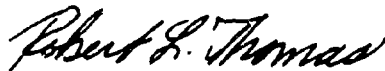
## VOLUME 3 - PREDICTION METHODS

by

A. B. Willoughby - C. Wilton  
and J. Mansfield

URS Research Company  
1811 Trousdale Drive  
Burlingame, California 94010

This report has been reviewed and approved.



ROBERT L. THOMAS  
Program Manager  
Liquid Propellant Blast Hazards Program  
Solid Rocket Division  
Air Force Rocket Propulsion Laboratory

## CONTENTS

<u>Section</u>		<u>Page</u>
1	INTRODUCTION . . . . .	1-1
2	REVIEW OF PROJECT PYRO . . . . .	2-1
3	PYRO BLAST PREDICTION METHOD FOR $\text{LO}_2/\text{RP-1}$ AND $\text{LO}_2/\text{LH}_2$ . . .	3-1
4	PYRO BLAST PREDICTION METHOD FOR $\text{N}_2\text{O}_4/50\% \text{N}_2\text{H}_4 - 50\% \text{UDMH}$ .	4-1
	Generalized Configuration . . . . .	4-1
5	EXAMPLES OF USE AND EXPERIMENTAL VERIFICATION OF PREDICTION METHOD . . . . .	5-1
6	HEAT TRANSFER HAZARD . . . . .	6-1
Appendix A	LIQUID PROPELLANT EXPLOSION PHENOMENA IN RELATION TO TNT . .	A-1
Appendix B	PEAK OVERPRESSURE VS DISTANCE AND POSITIVE-PHASE IMPULSE VS DISTANCE REFERENCE CURVES . . . . .	B-1

Section 1  
INTRODUCTION

The primary purpose of this document is to present a generalized method for predicting the blast and thermal environment resulting from explosions of the three most common liquid propellant combinations:

- Liquid oxygen/RP-1 ( $\text{LO}_2/\text{RP-1}$ )
- Liquid oxygen/liquid hydrogen ( $\text{LO}_2/\text{LH}_2$ )
- Nitrogen tetroxide/50% hydrazine - 50% unsymmetrical dimethylhydrazine - ( $\text{N}_2\text{O}_4/50\% \text{N}_2\text{H}_4-50\% \text{UDMH}$ )

The blast prediction method takes into account the fact that the explosive potential of a given liquid propellant combination in accidental failures is not a unique value, but depends on the manner in which the propellants are brought together during the failure process and on the time of ignition. Specifically, the method provides a means for predicting the blast environment as a function of the following system characteristics:

- Tank configuration
- Propellant type
- Propellant weight
- Nature of failure mode
- Ignition time

The thermal environment prediction is limited to the characteristics for each of the propellant combinations, partly because of the more limited data available and partly because the thermal characteristics are less dependent on the details of the failure conditions than are the blast characteristics.

It should be emphasized that the purpose of the prediction method presented in this section is to provide a means for predicting the explosion environment as a function of the various controlling parameters. As noted, the

cryogenic propellant combinations can have a wide range of explosive yield values, depending on the manner in which the propellants come into contact with each other and mix and on mixing time available before ignition. Thus, in order to use the prediction method for any given vehicle, it is necessary to conduct a detailed failure mode analysis to establish the credible failure modes and the credible ranges in values for the controlling parameters.

Included in this volume are:

Section 2. A brief summary of the general scope and the types of results obtained from the Project PYRO program. (For more details the reader is referred to Volume 1, the Technical Documentary Report on Project PYRO.)

Section 3. The blast prediction method for the cryogenic propellant combinations.

Section 4. The blast prediction method for the hypergolic propellant combination.

Section 5. Examples demonstrating the use of the cryogenic blast prediction method. Where possible the cases have been selected to correspond to actual full-scale or large-scale failure incidents or tests. In all cases where comparisons are made, the experimental results were not used in the basic derivation of the prediction method.

Section 6. Thermal prediction method.

Appendix A. A discussion of liquid propellant explosion phenomena in relation to TNT.

Appendix B. TNT reference overpressure and impulse versus distance curves.

Section 2  
REVIEW OF PROJECT PYRO

The objective of Project PYRO was to develop a reliable philosophy for predicting the credible damage potential which may be experienced from the accidental explosion of liquid propellants during launch or test operations of military missiles or space vehicles.

Such information is required for the siting of static test stands and launch facilities, for defining hazard envelopes, for launch operations, etc.

The PYRO program included experimental determination of the blast and thermal environments resulting from various types of propellant mixtures for the three liquid propellant combinations;  $N_2O_4/50\% N_2H_4 - 50\%$  UDMH,  $LO_2/RP-1$ , and  $LO_2/LH_2$ . Propellant weights up to about 100,000 lb were used for the cryogenic combinations and up to 1,000 lb for the hypergolic combination.

The generalized test conditions used were selected to simulate the important classes of propellant interaction, i.e., the manner in which the two propellants come into contact with each other and mix during an accidental failure. The ways in which the propellants can mechanically interact with each other are dependent on the initial conditions of the propellants at the start of the interaction and on the nature of the boundary conditions which control or confine the flow of propellants during the spillage and mixing process. The two major boundary conditions selected for testing were confinement by the missile and confinement by the ground surface.

The confinement-by-the-missile (CBM) condition is intended to simulate the general case where failure occurs in the intertank bulkhead and all propellant mixing is confined within the tankage. The initial conditions of primary concern for this case are the size of the opening in the intertank bulkhead, the length-to-diameter ratio of the tankage, the ullage volume, and the pressure rise to cause tank rupture.

The confinement-by-the-ground-surface (CBGS) condition simulates the case where the propellants spill out of the tankage and mix on the ground surface. Major emphasis in the program has been placed on a flat ground surface, although a limited amount of data was obtained for other conditions. The initial conditions of primary concern for this boundary condition are the velocities, shapes, and relative orientation of the propellant masses at the start of their interaction.

Conceptually, propellant mixing can also occur without confinement, i.e., after the propellants spill out of the tankage but before they reach the ground. Such free-fall mixing was not included in the program, however, because of the small amount of mixing anticipated. Unless there is a large velocity difference between the two propellants (which is unlikely for massive failures near the ground), there are no significant forces holding the two masses together, and even a small pressure generated by vaporization or reaction at the interface between the two masses will be sufficient to separate them and minimize mixing.

Although the generalized test conditions used resemble some actual failure modes, the intent in the program was not to investigate all credible combinations of tankage configuration, failure mode, and site geometry; there is an almost infinite number of such combinations. Rather, it was reasoned that many of these combinations would lead to similar propellant interactions and that study of several basic propellant interaction modes would be sufficient to provide a basis for evaluations or predictions under a variety of failure conditions.

The basic blast data obtained from these tests were peak overpressure and positive-phase impulse, both as a function of distance from the propellant explosion. Equivalent explosive weights at each measurement distance were determined separately for peak overpressure and positive-phase impulse, using standard TNT surface burst reference curves. Characteristically the TNT equivalent weights computed from these data vary both as a function of the shock wave parameter used (peak overpressure or positive-phase impulse) and the distance from an explosion. At long distances, however, the equivalent weights tend to approach an equal and constant value, which has been defined as the terminal



equivalent weight (when expressed in pounds of TNT) or terminal yield (when expressed as a percent of the total propellant weight).

The yield values based on peak overpressure generally tend to increase with increasing distance from the explosion until the terminal yield value is reached. The yield values based on positive-phase impulse generally tend to decrease with increasing distance until the terminal yield value is reached.

Thermal data obtained from the tests included total heat flux, gas temperatures, and radiant heat flux.

## Section 3

PYRO BLAST PREDICTION METHOD FOR  $\text{LO}_2/\text{RP-1}$  AND  $\text{LO}_2/\text{LH}_2$ 

In setting up the prediction method, it was recognized that there would likely be a wide variety of users for the method and that there would be various levels of detail desired in the output. Accordingly, the basic procedure was designed to provide the most detailed information possible about the blast environment within the current state of knowledge regarding liquid propellant explosives, but in a format that would also permit less detailed information to be obtained in a convenient fashion.

For the purposes of predicting the loading and response of objects to blast waves, it is normally sufficient to specify the peak overpressure (P) and positive-phase impulse (I) in the blast wave.\*

Thus the basic objective of the prediction method was to provide a means for determining P and I as a function of

distance - D

propellant weight - W

characteristics of missile or space vehicle system such as propellant type, tankage (and test site) configuration, and failure mode.

The basic steps in using the prediction method are:

1. Conduct engineering analysis of specific system to determine credible failure modes.
2. Determine for each credible failure mode the general sequence of events up to time of ignition, including gross space-time history of propellants.
3. Based on the postulated propellant space-time history, select the appropriate generalized PYRO mixing mode.

---

\* In the remainder of this volume, "peak-overpressure" and "positive-phase impulse" are referred to as "overpressure" and "impulse."

4. Estimate expected values (or ranges of values) of controlling parameters for each mixing mode.
5. Enter graph(s) for appropriate propellant type and mixing mode with values of other parameters and obtain terminal yield values.
6. Enter reference TNT pressure and impulse distance curves (given in Appendix B), using equivalent TNT weight determined from terminal yield to obtain pressure and impulse values at a given distance.
7. Enter tables for appropriate propellant type with scaled distance value and obtain appropriate correction factor for impulse. (For scaled distances less than  $2 \text{ ft}^2/\text{lb}^{1/3}$  see qualifying comments at end of Appendix A.)

The prediction method is presented in a series of charts (Figs. 3-1 through 3-5). Figure 3-1 shows the relation between the generalized PYRO mixing modes and typical full-scale failure modes to assist in the selecting of the appropriate mixing mode.

The equations relating explosive yield to ignition time in the prediction method were extrapolated to full scale by using the following postulated scaling relationship. Explosive yield (in percent of the total propellant weight) is independent of the propellant weight, providing the time of ignition is scaled by the cube root of the propellant weight, i.e.,  $y = t/W^{1/3}$ . This scaling relationship was postulated on the basis of the best available information concerning the physical phenomena involved in the propellant mixing and explosion processes. The initial check of scaling was made between test results from the 200 and 1,000 lb scales, and the results for all cases, except those for the  $\text{LO}_2/\text{RP-1}$  condition, were consistent with the postulated scaling.\* (These comparisons involved 200- and 1,000-lb tests.) Later a limited number of tests were conducted in the range from 25,000- to 100,000-lb, which also showed consistency with the postulated scaling. These larger scale comparisons are given in Section 5.

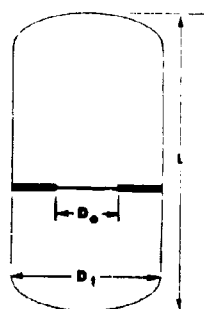
\* For the  $\text{LO}_2/\text{RP-1}$  CBM case, the results indicated a moderate decrease in yield with increasing weight up to about 10,000 lb. Above this weight the results were consistent with the postulated scaling.

TYPICAL FULL-SCALE FAILURE MODES	PYRO MIXING MODES	PREDICTION PROCEDURE
<b>BULKHEAD RUPTURE</b>  Failure occurs in the intertank bulkhead and all propellant mixing is confined within the tankage.	<b>CBM • CONFINEMENT BY MISSILE</b>  Controlling Parameters:  $T$ PROPELLANT MIXING TIME - msec Time between start of mixing and ignition. $W$ TOTAL PROPELLANT WEIGHT - lb $L/D$ LENGTH-TO-DIAMETER RATIO OF PROPELLANTS $D_o/D_i$ INTERTANK BULKHEAD OPENING RATIO Ratio of diameter of opening in intertank bulkhead to tank diameter. $V_u$ TANKAGE ULLAGE VOLUME Percent of total tankage volume. <sup>(1)</sup> $\Delta P_r$ TANK RUPTURE PRESSURE DIFFERENTIAL - psi Burst pressure minus initial pressure. <sup>(1)</sup>  <sup>(1)</sup> Not needed for LO <sub>2</sub> /LH <sub>2</sub> .	LO <sub>2</sub> /RP-1 - See Fig. 3-2 LO <sub>2</sub> /LH <sub>2</sub> - See Fig. 3-3 (top)
<b>OVERPRESSURIZATION-SEAM RIP AND LOW-ALTITUDE FALLBACK</b>  Propellants spill out of the vehicle and mixing occurs on the ground surface. Impact velocities $\leq 140$ ft/sec.  <ul style="list-style-type: none"> <li>Massive tankage rupture: propellants released through essentially full cross section of tankage, both tanks opened at about the same time.</li> <li>Same as I, but release of top propellant from tankage is considerably delayed over bottom.</li> <li>Propellants released through openings significantly smaller than tank cross section.</li> </ul>	<b>CBGS • CONFINEMENT BY GROUND SURFACE</b>  Controlling Parameters:  $I$ PROPELLANT MIXING TIME - sec Time between propellant contact on ground surface and ignition. $W$ TOTAL PROPELLANT WEIGHT - lb $V$ PROPELLANT VELOCITY - ft/sec $FT$ FAILURE SUBTYPE  I ..... I II ..... II III ..... III	LO <sub>2</sub> /RP-1 - See Fig. 3-4 LO <sub>2</sub> /LH <sub>2</sub> - See Fig. 3-5
<b>POWERED IMPACT AND HIGH-ALTITUDE FALLBACK</b>  Impact velocities from 140 to 600 ft/sec. Ignition assumed to occur at impact.	<b>HVI • HIGH-VELOCITY IMPACT</b>  Controlling Parameters:  $V$ IMPACT VELOCITY - ft/sec $GS$ NATURE OF GROUND SURFACE Hard: Essentially no penetration of surface by impacting tankage. (Example: concrete and rock.) Soft: Essentially complete penetration of surface by impacting tankage. (Example: water.)	All Propellants - See Fig. 3-3 (bottom)

Fig. 3-1. Relation Between Typical Full-scale Failure Modes and PYRO Mixing Modes

**LO<sub>2</sub>/RP-1: CBM****step 1** DETERMINE PARAMETER VALUES

- T** PROPELLANT MIXING TIME - msec  
Time between start of mixing and ignition  
(If unknown consider  $T_{max}$ )
- W** TOTAL PROPELLANT WEIGHT - lb
- L/D** LENGTH-to-DIAMETER RATIO OF PROPELLANTS
- D<sub>o</sub>/D<sub>t</sub>** INTERTANK BULKHEAD OPENING RATIO  
Ratio of diameter of opening in intertank  
bulkhead to tank diameter.  
(If opening diameter not circular use diameter  
of circle having same opening area).
- V<sub>U</sub>** TANKAGE ULLAGE VOLUME - percent  
of total tankage volume
- ΔP<sub>r</sub>** TANK RUPTURE PRESSURE DIFFERENTIAL - psi  
(burst pressure minus initial pressure)

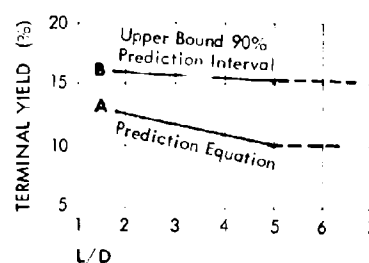
**step 2** DETERMINE PROCEDURE

PROCEDURE	W - lb	D <sub>o</sub> /D <sub>t</sub>	TIME
A	> 10,000	< 0.45	Unknown
B	> 10,000	< 0.45	Known
C	< 10,000	< 0.45	Either
C	any value	> 0.45	Either

**step 3** OBTAIN TERMINAL YIELD (Y)**procedure**

- Using L/D value, obtain Y<sub>S</sub> from curve A, Figure A-1.  
Y<sub>S</sub> - terminal yield at tank rupture  
for V<sub>U</sub> = 10%, ΔP<sub>r</sub> = 85 psi.

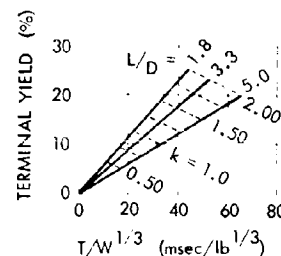
Figure A-1

**B**

- With V<sub>U</sub> and ΔP<sub>r</sub> values, determine k value from Procedure A.

With k and L/D values, enter Figure B-1 and allowable T/W<sup>1/3</sup> value. Compare with T/W<sup>1/3</sup> less than 5 msec/lb<sup>1/3</sup>.

Figure B-1



- Enter L and W to determine TERMINAL YIELD

**C**

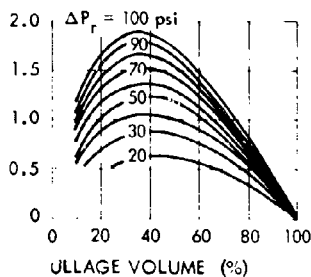
- If W < 10,000 lb. and D<sub>o</sub>/D<sub>t</sub> < 0.45, obtain yield value Y from general predictive Procedure A or B as appropriate.

TERMINAL YIELD is given by:  $Y(1 + \frac{21}{W})$

YIELD (Y) AND UPPER 90% PREDICTION VALUE ( $Y_{90}$ )

- Enter Figure A-2 with the  $\Delta P_r$  and the  $V_u$  values to obtain a  $k$  value. Multiply  $Y_S$  times  $k$  to get TERMINAL YIELD (Y). This is what would be obtained if ignition occurred at time of tank rupture, the latest possible time for this case.

Figure A-2



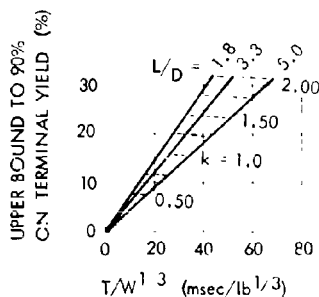
- Using  $L/D$  value, obtain  $Y_{S-90}$  from curve B in Figure A-1.
- Multiply  $Y_{S-90}$  by  $k$  value to get UPPER 90% PREDICTION VALUE ( $Y_{90}$ ). (There is a 90% probability that the yield will be below this value).

• Use same  $T/W^{1/3}$  value and Figure B-2

Figure B-1 and obtain maximum yield with  $T/W^{1/3}$  value derived

- to determine UPPER 90% PREDICTION VALUE ( $Y_{90}$ ) for terminal yield.

Figure B-2



- Enter Figure B-1 again and with  $L/D$  value determine TERMINAL YIELD (Y).

- If  $D_o/D_i > 0.45$ , terminal yield is given by the following equation for a  $V_u = 10\%$  and a  $\Delta P_r = 85$  psi.

$$Y_1 = \frac{T}{W^{1/3}} \left( 1 + \frac{217}{W} \right) (0.59 - 0.092 L/D)$$

Estimated max. allowable  $T/W^{1/3}$  values:

$L/D$	$(T/W^{1/3})_{max}$
1.8	43
5.0	57

To correct for differences in standard conditions, multiply  $(T/W^{1/3})_{max}$  values by  $k$  factor given in Figure A-2.

## step 4 DETERMINE PRESSURE AND IMPULSE VALUES

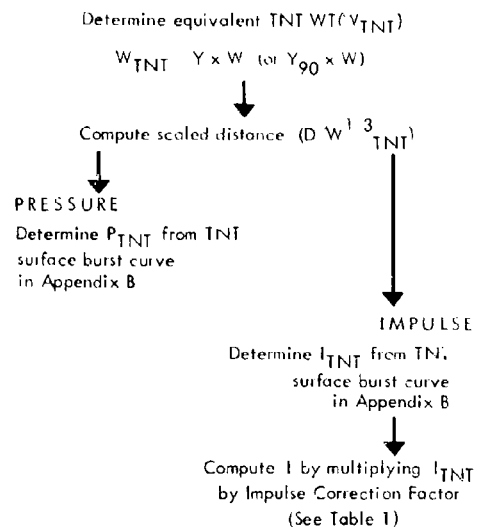


TABLE 1

SCALED DISTANCE RANGE	CORRECTION FACTOR
$> 3$	1.3
$\leq 3$ (ft, lb <sup>1/3</sup> )	2.0

Fig. 3-2.

# $LO_2/LH_2$ : CBM

## step 1 DETERMINE PARAMETER VALUES

- T** PROPELLANT MIXING TIME - msec  
Time between start of mixing and ignition  
(If unknown, consider  $T_{max}$ ).
- W** TOTAL PROPELLANT WEIGHT - lb
- L/D** LENGTH-TO-DIAMETER RATIO OF PROPELLANTS
- $D_o/D_t$**  INTERTANK BULKHEAD OPENING RATIO  
Ratio of diameter of opening in intertank bulkhead to tank diameter.  
(If opening diameter not circular, use diameter of circle having same opening area).

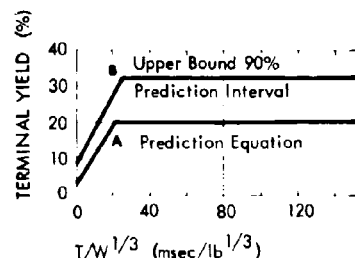
## step 2 DETERMINE PROCEDURE

PROCEDURE	L/D	$D_o/D_t$
A	$> 5.0$	All values
A	$\geq 1.8$	$\leq 0.45$
B	$\leq 5.0$	$\geq 0.45$

procedure  
A

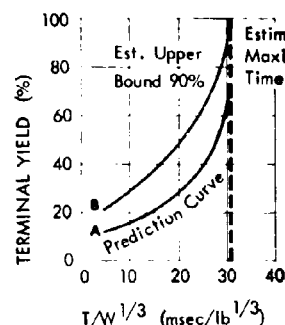
## step 3 OBTAIN TERMINAL YIELD (Y) AND UPPER 90% PRE

- Compute  $T/W^{1/3}$  from input data and determine TERMINAL YIELD from curve A.



B

- Compute  $T/W^{1/3}$  from input data and determine TERMINAL YIELD from curve A.



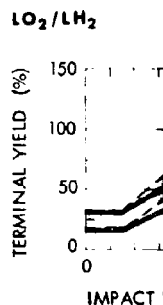
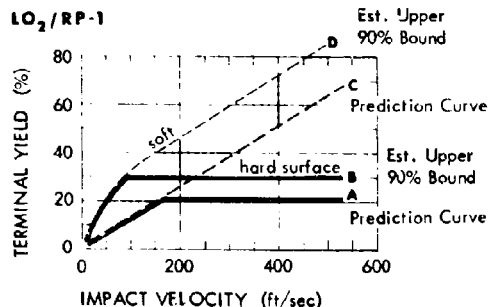
# HIGH-VELOCITY IMPACT: all propellants

## step 1 DETERMINE PARAMETER VALUES

- V** IMPACT VELOCITY - ft/sec
- GS** NATURE OF GROUND SURFACE
- Hard: Essentially no penetration of surface by impacting tankage. (Example - concrete and rock).
- Soft: Essentially complete penetration of surface by impacting tankage. (Example - water).

## step 2 OBTAIN TERMINAL YIELD (Y) AND UPPER 90% PRE

- From the graphs of Terminal Yield vs Impact Velocity for  $LO_2/RP-1$  and determine TERMINAL YIELD (curves A and C) and UPPER 90% PREDIC for appropriate propellant type.

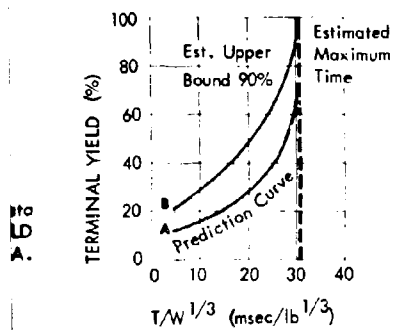


A

Figure 1 is a line graph showing the relationship between Terminal Yield (%) and  $T/W^{1/3}$  (msec/lb<sup>1/3</sup>) for a 90% Upper Bound Prediction Interval. The y-axis represents Terminal Yield (%) from 0 to 40. The x-axis represents  $T/W^{1/3}$  (msec/lb<sup>1/3</sup>) from 0 to 160. Three data series are plotted: 'Upper Bound 90%' (a solid line with square markers), 'Prediction Interval' (a shaded region), and 'Prediction Equation' (a solid line with triangle markers). The 'Upper Bound 90%' line starts at approximately (0, 10), rises to (20, 35), and then levels off at 35% for  $T/W^{1/3} > 20$ . The 'Prediction Interval' is a shaded region bounded by two lines that both start at (0, 10) and level off at different yield values (approximately 20% and 33%) for  $T/W^{1/3} > 20$ . The 'Prediction Equation' line starts at (0, 10), rises to (20, 20), and then levels off at 20% for  $T/W^{1/3} > 20$ .

$T/W^{1/3}$ (msec/lb <sup>1/3</sup> )	Upper Bound 90% Yield (%)	Prediction Interval Lower Bound Yield (%)	Prediction Interval Upper Bound Yield (%)	Prediction Equation Yield (%)
0	10	10	10	10
20	35	20	33	20
40	35	20	33	20
80	35	20	33	20
120	35	20	33	20
160	35	20	33	20

(There is a 90% probability that the yield will be below this value.)



- Determine UPPER 90% PREDICTION VALUE from curve B.

Figure 1 is a line graph showing Terminal Yield (%) on the y-axis (0 to 150) versus Impact Velocity (ft/sec) on the x-axis (0 to 600). Two curves are plotted: a dashed line labeled 'soft' and a solid line labeled 'hard surface'. Both curves show an increase in yield with impact velocity. The 'soft' curve is consistently higher than the 'hard surface' curve. Both curves are labeled 'Prediction Curve' and 'Est. Upper 90% Bound' at 600 ft/sec.

Impact Velocity (ft/sec)	Terminal Yield (%) - soft	Terminal Yield (%) - hard surface
0	~25	~15
100	~45	~30
200	~70	~50
300	~100	~75
400	~130	~100
500	~160	~125
600	~190	~150

Compute  $I$  by multiplying  $I_{\text{INT}}$   
by Impulse Correction Factor  
(See Table I)

SCALED DISTANCE RANGE	CORRECTION FACTOR
$\geq 5$	1.4
$\leq 5$ (ft/lb <sup>1/3</sup> )	2.0

3-7



# LO<sub>2</sub>/RP-1: CBGS

## step 1 DETERMINE PARAMETER VALUES

- T** PROPELLANT MIXING TIME - sec  
(Time between propellant contact on ground surface and ignition).  
 $T_T$  - top propellant  
 $T_B$  - bottom propellant  
If unknown, consider  $T_{max}$ .
- W** TOTAL PROPELLANT WEIGHT - lb
- V** PROPELLANT IMPACT VELOCITY - ft/sec
- FT** FAILURE SUBTYPE  
I Fallback -  
Massive tankage rupture,  
propellants released through essentially  
full cross section of tankage, both tanks  
opened at about the same time.  
 $T, T_B, V$  velocity of interface  
between propellants
- II Fallback -  
Same as I, but release of top propellant  
from tankage is considerably delayed  
over bottom.
- III Non-Massive Tank Rupture -  
Propellants released through openings  
significantly smaller than tank cross section.

## step 2 DETERMINE PROCEDURE

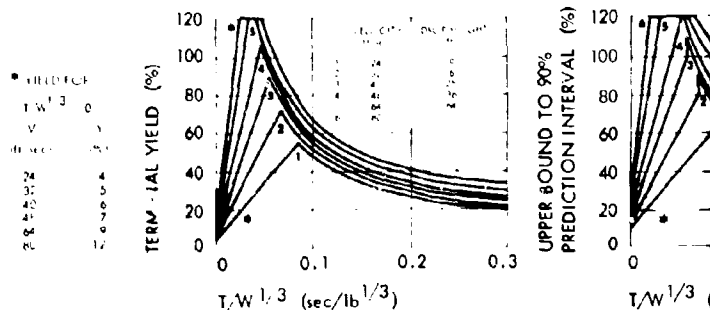
PROCEDURE	TIME	FAILURE SUBTYPE
A	Known	I
B	Known	II
C	Known	III
D	Unknown	I, II, III

## step 3 OBTAIN TERMINAL YIELD (Y) AND UPPER 90% PREDICTION INTERVAL

procedure

A

- Compute  $T/W^{1/3}$  from input data. With this value and V value, determine TERMINAL YIELD.
- With  $T/W^{1/3}$  and V determine UPPER 90% PREDICTION INTERVAL.



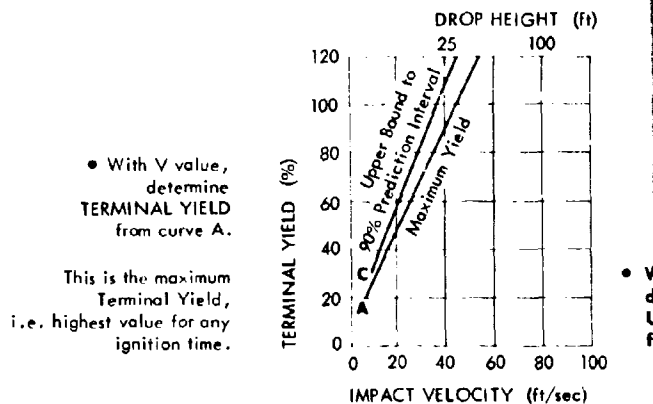
B

- Compute from following equation:  $Y = Y_S \frac{W_{LO_2} + W_{RP-1}}{W_T}$   
where . . .  
 $W_{LO_2}$  = total LO<sub>2</sub> weight  
 $W_{RP-1}$  = weight of RP-1 overlapped  
 $W_T$  = total weight  
 $Y_S$  = specific yield (right axis of graph A)
- Compare yield with value given in Procedure A (use smallest yield value, but in no case use less than Procedure A).
- ESTIMATE UPPER 90% PREDICTION VALUE by increasing yield estimate by 50% using Procedure A.

C

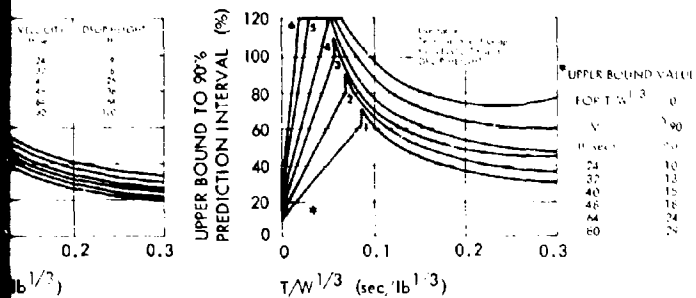
- Use same procedure as in A, but use  $W_f$  in place of W for computing  $T/W^{1/3}$  weight of both propellants on the ground at time of ignition.  
TERMINAL YIELD VALUE is multiplied by  $W_f$  (rather than W) in Step 4 to. In no case should an equivalent weight in lb be used that is less than given.

D



FIELD (Y) AND UPPER 90% PREDICTION VALUE (Y<sub>90</sub>)

- Input data.  
value,  
FIELD.
- With  $T/W^{1/3}$  and V value,  
determine UPPER 90% PREDICTION VALUE.



$$Y = Y_S \frac{W_{LO_2} + W_{RP-1}}{W_T}$$

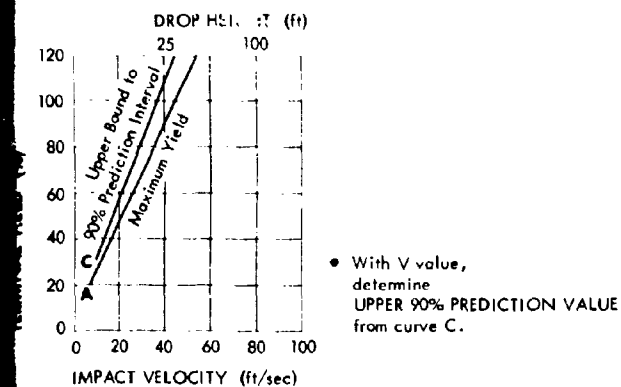
- Weight of RP-1 overlaps.
- $W_T$  - total weight of propellants in vehicle  
 $Y_S$  = specific yield and is obtained from Table 2 (right column) using an oxidizer-to-fuel ratio of  $W_{LO_2} / W_{RP-1}$ .

Procedure A  
 value, in no case use less than Procedure A gives for  $c \cdot T/W^{1/3} = 0$ .

VALUE by increasing yield estimate by same ratio as upper bound is to yield

Use  $W_f$  in place of  $W$  in computing  $T/W^{1/3}$  where  $W_f$  is the estimated weight in lb of the ground at time of impact.

Multiplied by  $W_f$  (rather than  $W$ ) in Step 4 to get equivalent weight in lb. Weight in lb to be used that is less than given in Procedure A with a  $T/W^{1/3} = 0$ .



- With V value,  
determine  
UPPER 90% PREDICTION VALUE  
from curve C.

## step 4 DETERMINE PRESSURE AND IMPULSE VALUES

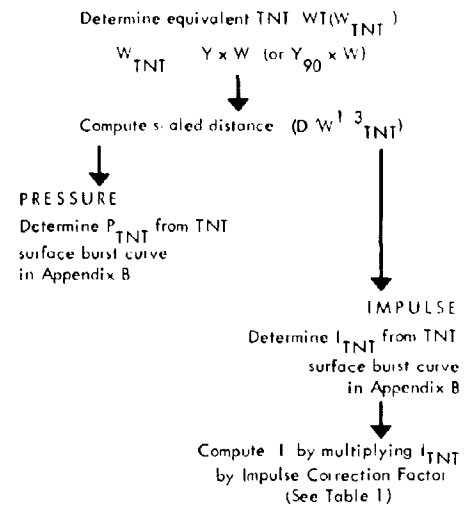


TABLE 1

SCALED DISTANCE RANGE	CORRECTION FACTOR
> 3 (ft. lb <sup>1/3</sup> )	1.3
≤ 3	2.0

TABLE 2	LO <sub>2</sub> /RP-1 Ratio	Y <sub>S</sub> (%)
	1.5	93
	2.0	113
	2.5	126
	3.0	132
	3.5	123
	4.0	115
	4.5	105
	5.0	96
	6.0	83
	7.0	70
	8.0	59
	10.0	43
	12.0	31
	14.0	22
	16.0	16
	18.0	12

Fig. 3-4.

LO<sub>2</sub>/LH<sub>2</sub>: CBGS

step1 DETERMINE PARAMETER VALUES

- T PROPELLANT MIXING TIME - sec  
(Time between propellant contact on ground surface and ignition).  
 $T_T$  - top propellant  
 $T_B$  - bottom propellant  
If unknown, consider  $T_{max}$ .
- W TOTAL PROPELLANT WEIGHT - lb
- V PROPELLANT VELOCITY - ft/sec
- FT FAILURE SUBTYPE
- I Fallback -  
Massive tankage rupture, propellants released through essentially full cross section of tankage, both tanks opened at about the same time.  
 $T = T_B$ ; V = velocity of interface between propellants
- II Fallback -  
Same as I, but release of top propellant from tankage is considerably delayed over bottom.
- III Non-Massive Tank Rupture -  
Propellants released through openings significantly smaller than tank cross section.

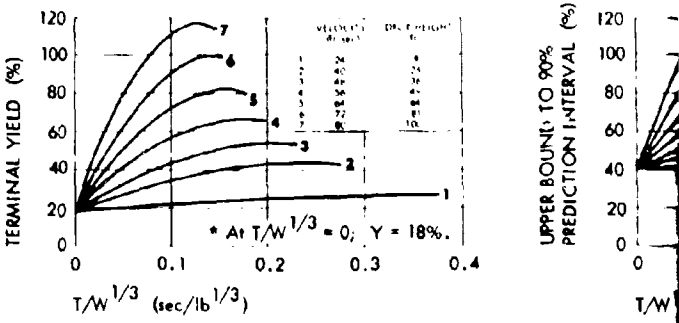
step2 DETERMINE PROCEDURE

PROCEDURE	TIME	FAILURE SUBTYPE
A	Known	I, II
B	Known	III
C	Unknown	I, II, III

procedure

step3 OBTAIN TERMINAL YIELD (Y) AND UPPER 90% PRED

- Compute  $T/W^{1/3}$  from input data and determine TERMINAL YIELD.
- With  $T/W^{1/3}$  as determine UPPER 90% PRED



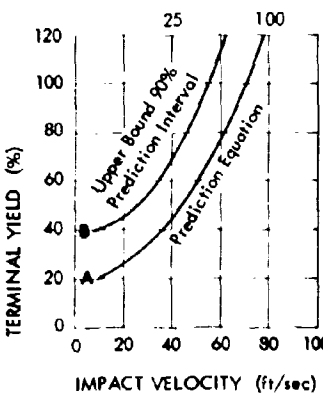
B

- Use same procedure as in A, but use  $W_f$  in place of W for computing weight of both propellants on the ground at time of ignition.

TERMINAL YIELD VALUE is multiplied by  $W_f$  (rather than W) in S. In no case should an equivalent weight in lb be used that is less with a  $T/W^{1/3} = 0$ .

C

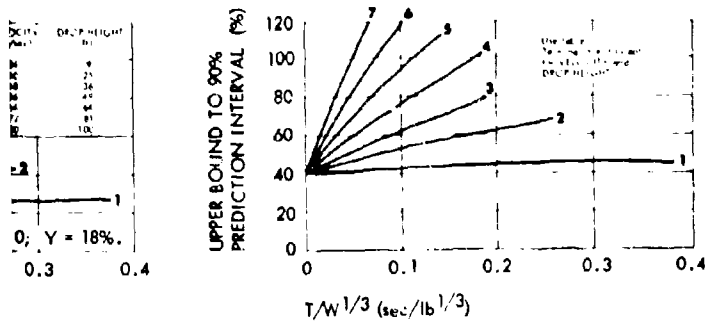
- With V value, determine TERMINAL YIELD from curve A.
- This is the maximum Terminal Yield, i.e. highest value for any ignition time.





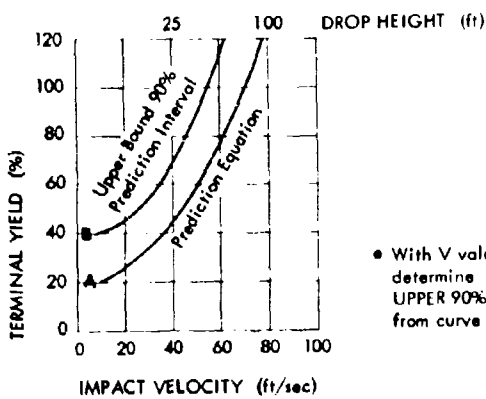
LD (Y) AND UPPER 90% PREDICTION VALUE ( $Y_{90}$ )

• With  $1/W^{1/3}$  and V value,  
determine UPPER 90% PREDICTION VALUE.



Use  $W_f$  in place of  $W$  for computing  $T/W^{1/3}$  where  $W_f$  is the estimated weight on the ground at time of ignition.

Is multiplied by  $W_f$  (rather than  $W$ ) in Step 4 to get equivalent weight in lb. Equivalent weight in lb. to be used that is less than given in Procedure A



#### step 4 DETERMINE PRESSURE AND IMPULSE VALUES

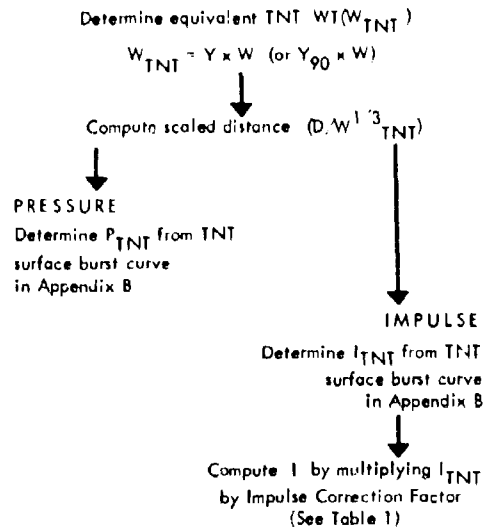


TABLE 1

SCALED DISTANCE RANGE	CORRECTION FACTOR
$\geq 5$	1.4
$\leq 5$ (ft/lb <sup>1/3</sup> )	2.0

Fig. 3-5.

## Section 4

PYRO BLAST PREDICTION METHOD FOR  $N_2O_4/50\% N_2H_4$  - 50% UDMH

The general approach used in the prediction method for  $N_2O_4/50\% N_2H_4$  - 50% UDMH is similar to that for the cryogenic propellant combinations. The procedures, however, are considerably simpler because time of ignition is not a controlling parameter and because the generally low magnitudes of the yields made it possible to eliminate much of the parameter variations needed for the cryogenic propellant combinations.

The basic steps in the prediction procedure are:

1. Identify the PYRO generalized configuration from the list given below.
2. Follow specified procedures to determine terminal yield and pressure and impulse correction factors.

## GENERALIZED CONFIGURATION

1. Static Test Stand
  - a. Assumes tank and tank support structure are strong enough to eliminate fallover case and no large explosive donor (i.e., another stage) is present.
  - b. Applicable PYRO mixing modes are: diaphragm rupture (confinement by the missile); spill; small explosive donor (i.e.,  $\leq 0.5\%$  of the propellant weight), and tower drop.
2. Launch Pad
  - a. Pre-launch

Applicable PYRO mixing modes are: diaphragm rupture, spill, small explosive donor, and tower drop.
  - b. Launch

Applicable PYRO mixing modes include those indicated for pre-launch as well as large explosive donor (i.e., another stage) and low-velocity impact ( $\sim 140$  ft/sec). Does not include high-velocity impact (either from high-altitude fallback or powered impact).

### 3. Post-Launch

#### a. In-Flight

No data were obtained for this case during the PYRO program; however, in the absence of a spill surface, there seems to be no possible way for the failure mode to be more severe than the launch case. It is recommended that this value be used.

#### b. Ground Impact

Applicable PYRO mixing mode is high-velocity impact.

Table 4-1 gives the estimated upper limit for the terminal yield for each of the PYRO generalized configurations. For all cases but the high-velocity impact condition, a single terminal yield value could be used. For this case the value shown in Table 4-1 is for the upper limit of velocity (600 ft/sec) and a curve of terminal yield vs velocity is given in Fig. 4-1 for use with lower impact velocities.

With the terminal yield for a specified failure mode established by use of Table 4-1 or Fig. 4-1, the next step in the prediction procedure is to determine the pressure and impulse correction factors. These are obtained from Fig. 4-2 by entering in the proper scaled distance. The propellant overpressure and impulse values are obtained by multiplying the overpressure and impulse values obtained from the surface burst TNT curves shown in Appendix B by these factors.

Table 4-1

TERMINAL YIELD ESTIMATES FOR  
SELECTED FACILITY AND APPLICATION MODES

FACILITY AND APPLICATION MODE	ESTIMATED UPPER LIMIT TO TERMINAL YIELD (%)
STATIC TEST STAND*	2
LAUNCH PAD	
• Pre-Launch*	2
• Launch**	5
POST-LAUNCH	
• In-Flight**	5
• High Velocity Impact	
Hard Surface	25
Soft Surface	60

\* If no small explosive donor (i.e., <1% of total propellant weight) is present a yield of 1.5 percent can be used.

\*\* If no large explosive donor (i.e., another stage) is present a yield of 3 percent can be used.

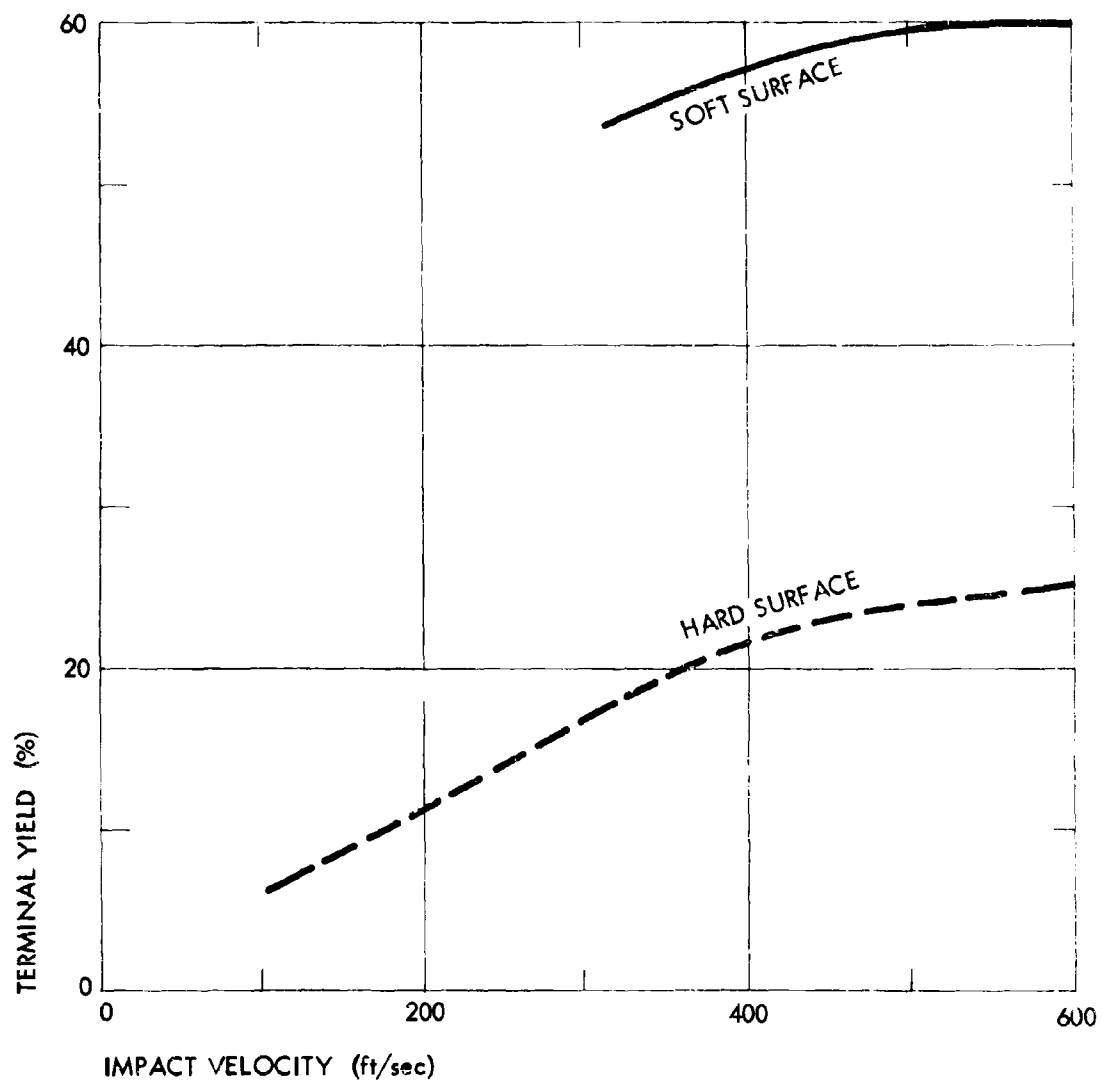


Fig. 4-1. Terminal Yield vs Impact Velocity for Hypergolic High-Velocity Impact



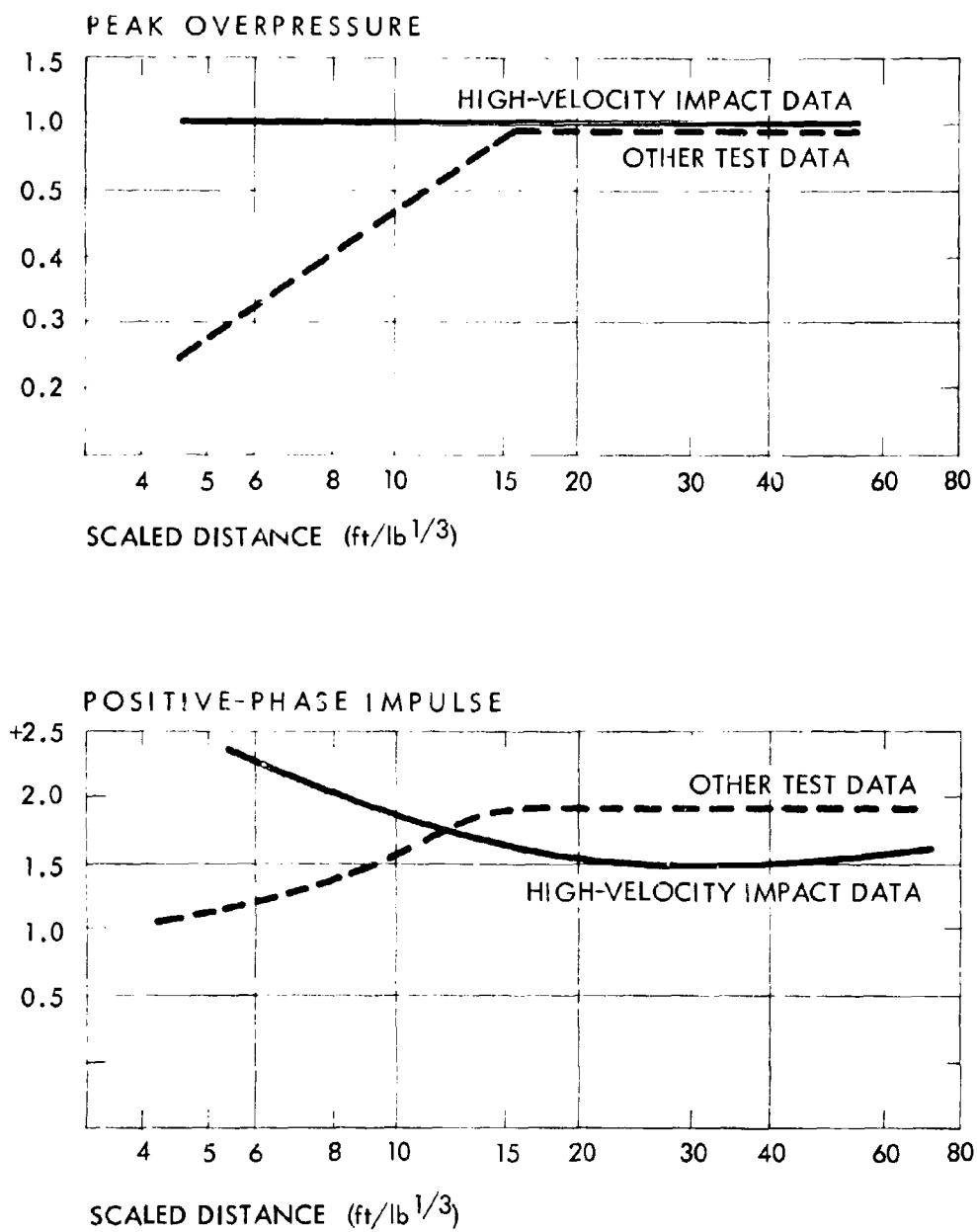


Fig. 4-2. Ratio of Upper Bound of Propellant Peak Overpressure and Positive Phase Impulse Data to Standard TNT Curve

## Section 5

EXAMPLES OF USE AND EXPERIMENTAL VERIFICATION  
OF PREDICTION METHOD

Examples illustrating the use of the prediction method are given in this section. The cases covered are listed below. Where possible the cases have been selected to correspond to actual full-scale or large-scale failure incidents or tests. In all cases where comparisons are made, the experimental results were not used in the basic derivation of the prediction method.

EXAMPLE NO.	PROPELLANT COMBINATION	FAILURE MODE	COMPARISON CASE	TYPE OF COMPARISON
1	LO <sub>2</sub> /RP-1	Bulkhead Rupture - Ignition Time Unknown	ATLAS 9C	Full-Scale Accident
2	LO <sub>2</sub> /RP-1	Bulkhead Rupture - Ignition Time Known	AFRPL TITAN I Test (No. 301)	Full-Scale Test
3	LO <sub>2</sub> /LH <sub>2</sub>	Bulkhead Rupture - Ignition Time Known	AFRPL SATURN S-IV Test (No. 62)	Full-Scale Test
4	LO <sub>2</sub> /RP-1	Fallback - Ignition Time Known	AFRPL 25,000-lb Test (No. 285)	Large-Scale Test
5	LO <sub>2</sub> /RP-1	Fallback - Ignition Time Unknown	None	None
6	LO <sub>2</sub> /LH <sub>2</sub>	Fallback - Ignition Known	AFRPL 25,000-lb Test (No. 228C)	Large-Scale Test
7	LO <sub>2</sub> /RP-1 LO <sub>2</sub> /LH <sub>2</sub>	Fallback - Ignition Time Known	AFRPL 1,200-lb Test (No. 295)	Small-Scale Test

1. BULKHEAD RUPTURE OF LO<sub>2</sub>/RP-1 VEHICLE ON LAUNCH PAD OR STATIC TEST STAND -  
IGNITION TIME UNKNOWN - CORRESPONDS TO PYRO CBM CASE

Assumed Conditions\*

$W = 240,000$  lb (weight of propellants when vehicle has normal full load of propellants)

$$L/D = 5$$

$$D_o/D_t \leq 0.45$$

$$V_u = 40\% \text{ at time of failure}$$

$$\Delta P_r = 30 \text{ psi}$$

Prediction Procedure (Refer to Fig. 3-2)

1. In accordance with step 2, Procedure A is selected.
2. Following step 3, a  $Y_S$  of 10% is selected from curve A of Fig. A-1 with the given  $L/D$  value of 5. Also a  $k$  of 0.9 is obtained from Fig. A-2 using  $\Delta P_r = 30$  psi and a  $V_u = 40\%$ . The predicted terminal yield value of 9% is then obtained by multiplying 0.9 times 10%.
3. Continuing with step 3, the upper 90% prediction bound is 14% ( $0.9 \times 15\%$ ).
4. Following step 4, an impulse correction factor of 1.3 is obtained for scaled distances of greater than  $3 \text{ ft/lb}^{1/3}$  and a value of 2 for scaled distances less than  $3 \text{ ft/lb}^{1/3}$ . With the derived explosive yield of 9% or 22,000 lb of TNT (for the 240,000 lb of propellant) this means that for actual distances greater than  $3 \times 22,000^{1/3} = 84$  ft, the impulse values obtained from standard TNT impulse-distance curves should be multiplied by 1.3. Similarly for distances less than 84 ft, the impulse value should be multiplied by 2.

\*  $W$  is total propellant weight;  $L/D$  is length-to-diameter ratio of propellants;  $D_o/D_t$  is ratio of the diameter of the opening in the bulkhead to the tank diameter;  $V_u$  is tankage ullage volume;  $\Delta P_r$  is tank rupture pressure differential.

Full-Scale Comparison

The case selected is believed to correspond to the Atlas 9C failure. The actual ullage volume at ignition in this case was unknown, but propellants were being pumped out of the vehicle for 30 to 60 sec prior to ignition, so that the ullage volume was clearly very much larger than the normal 5%. The measured yield from the failure was 10-12%, which compares quite favorably with the predicted value of 9% and the upper bound of 14%.

2. BULKHEAD RUPTURE OF LO<sub>2</sub>/RP-1 VEHICLE ON LAUNCH PAD OR STATIC TEST STAND - IGNITION TIME KNOWN - CORRESPONDS TO PYRO CBM CASE

Assumed Conditions

$$T = 840 \text{ msec}$$

$$W = 170,000 \text{ lb (weight of propellants when vehicle has normal full load of propellants)}$$

$$L/D = 4$$

$$D_o/D_t \leq 0.45$$

$$V_u = 50\% \text{ (corresponds to a propellant loading of about 55\% or 94,000 lb of propellant)}$$

$$\Delta P_r = 35 \text{ psi}$$

Prediction Procedure (Refer to Fig. 3-2)

1. In accordance with step 2, procedure B is selected.
2. Following step 3, a k value of 0.9 is obtained from Fig. A-2 by entering with a  $V_u = 50\%$  and a  $\Delta P_r = 35 \text{ psi}$ . Next a maximum allowable value of  $T/W^{1/3} = 27 \text{ msec/lb}^{1/3}$  is obtained from Fig. B-1 by using the k value of 0.9 and an  $L/D = 4$ . Since this is larger than the value computed from the input data,  $840/(170,000)^{1/3} = 15$ , the input value (being the smaller of the two) is selected and entered into Fig. B-1, with an  $L/D = 4$  to obtain a terminal yield = 6%.
3. Again using a  $T/W^{1/3} = 15$  and an  $L/D = 4$ , the upper 90% prediction value = 8% is obtained from the lower part of Fig. B-2.

Full-Scale Comparison

The case selected corresponds to the Titan I test conducted under the PYRO program (Test Number 301). The measured yield was 4% based on the 94,000 lb of propellant used or 2% on a fully loaded vehicle. The predicted value of 6% would be expected to be conservative (i.e., somewhat high) for this case because of the small size of the opening area in the inter-tank bulkhead, which amounted to only about 2% of the tank cross-sectional area. The prediction method was based on results with diaphragm openings equal to or greater than 20% of the tank cross-sectional area and was expected to be conservative for cases having much smaller openings.

3. BULKHEAD RUPTURE OF LO<sub>2</sub>/LH<sub>2</sub> VEHICLE ON LAUNCH PAD OR STATIC TEST STAND - IGNITION TIME KNOWN - CORRESPONDS TO PYRO CBM CASE

Assumed Condition

$$T = 183 \text{ msec}$$

$$W = 91,000 \text{ lb}$$

$$L/D = 1.8$$

$$D_o/D_t \leq 0.45$$

Prediction Procedure (Refer to Fig. 3-3)

1. In accordance with step 2, procedure A is selected.
2. Following step 3, a  $T/W^{1/3} = 4 \text{ msec/lb}^{1/3}$  is computed ( $183/91,000^{1/3}$ ), and a terminal yield of 6% is obtained by using this value with curve A.
3. An upper 90% prediction bound of 12% is obtained from curve B in the same manner.

Full-Scale Comparison

This case corresponds to the S-IV test conducted as part of Project PYRO (Test No. 62). The measured yield was 5%, which compares favorably with the predicted value of 6%.

4. FALLBACK OF LO<sub>2</sub>/RP-1 VEHICLE ON LAUNCH PAD - IGNITION TIME KNOWN - CORRESPONDS TO PYRO CBGS CASE

Assumed Condition\*

$$T = 0.465 \text{ sec}$$

$$W = 25,000 \text{ lb}$$

$$V = 44 \text{ ft/sec}$$

$$FT = I$$

Prediction Procedure (Refer to Fig. 3-4)

1. In accordance with step 2, procedure A is selected.
2. Following step 3, a  $T/W^{1/3} = 0.016 \text{ sec/lb}^{1/3}$  is computed ( $0.465/25,000^{1/3}$ ) and a terminal yield of 36% is obtained from this value and a  $V = 44$ .
3. Continuing with step 3, an upper 90% prediction bound of 46% is obtained in a similar fashion.

Large-Scale Comparison

This case corresponds to a 25,000-lb test (No. 285) conducted under the PYRO program. The measured yield was 37%, which compares very well with the predicted value of 36% and upper bound of 46%.

5. FALLBACK OF LO<sub>2</sub>/RP-1 VEHICLE ON LAUNCH PAD - IGNITION TIME UNKNOWN - CORRESPONDS TO PYRO CBGS CASE

Assumed Condition

$$W = 25,000 \text{ lb}$$

$$V = 44 \text{ ft/sec}$$

$$FT = I$$

\* V is impact velocity; FT is failure subtype.

Prediction Procedure (Refer to Fig. 3-4)

1. In accordance with step 2, procedure D is selected.
  2. Following step 3, a terminal yield value of 97% is obtained by using a  $V = 44$  ft/sec.
  3. Continuing with step 3, an upper 90% prediction bound of 120% is obtained in a similar fashion.
6. FALLBACK OF  $LO_2/LH_2$  VEHICLE ON LAUNCH PAD - IGNITION TIME KNOWN - CORRESPONDS TO PYRO CBGS CASE

Assumed Conditions

$$T = 0.365 \text{ sec}$$

$$W = 25,000 \text{ lb}$$

$$V = 44 \text{ ft/sec}$$

$$FT = I$$

Prediction Procedure (Refer to Fig. 3-5)

1. In accordance with step 2, procedure A is selected.
2. Following step 3, a  $T/W^{1/3} = 0.012 \text{ sec/lb}^{1/3}$  is computed ( $0.365/25,000^{1/3}$ ) and a terminal yield of 22% is obtained from this value and a velocity of 44.
3. Continuing with step 3, an upper 90% prediction bound of 42% is obtained in a similar fashion.

Large-Scale Comparison

This case corresponds to a 25,000-lb test (No. 288C) conducted under the PYRO program. The measured yield was 13%, somewhat under the predicted value of 22% but well within the uncertainty limits for this case, as evidenced by the difference between the expected value of 22% and the upper 90% bound of 42%.

7. FALLBACK OF TWO-STAGE VEHICLE (UPPER STAGE  $\text{LO}_2/\text{LH}_2$  - LOWER STAGE  $\text{LO}_2/\text{RP-1}$ )  
- IGNITION TIME KNOWN - CORRESPONDS TO PYRO CBGS CASE

Assumed Conditions

$W - \text{LO}_2/\text{RP-1 stage} = 1,000,000 \text{ lb}$

$W - \text{LO}_2/\text{LH}_2 \text{ stage} = 200,000 \text{ lb}$

$T = 5.4 \text{ sec}$

$V = 44 \text{ ft/sec}$

$FT = 1$

Prediction Procedure -  $\text{LO}_2/\text{RP-1}$  Stage (Refer to Fig. 3-4)

1. In accordance with step 2, procedure A is selected.
2. Following step 3, a  $T/W^{1/3} = 0.054$  is computed ( $5.4/1,000,000^{1/3}$ ), and a terminal yield of 93% is obtained from this value and a  $V = 44$ . This gives an equivalent explosive weight of 930,000 lb ( $93\% \times 1,000,000 \text{ lb}$ ).

Prediction Procedure -  $\text{LO}_2/\text{LH}_2$  Stage (Refer to Fig. 3-5)

1. In accordance with step 2, procedure A is selected.
2. Following step 3, a  $T/W^{1/3} = 0.092$  is computed ( $5.4/200,000^{1/3}$ ), and a terminal yield of 37% is obtained using this value and a  $V = 44$ . This gives an equivalent explosive weight of 74,000 lb ( $37\% \times 200,000 \text{ lb}$ ).

Combined Yield Predictions

Sum of equivalent explosive weights is 1,004,000 lb ( $930,000 + 74,000$ ) giving a terminal yield for the combination of 84% ( $100 \times 1,004,000/1,200,000$ ).

Experimental Comparison

No full-scale or large-scale data are available for comparison with this case; however, one 1,200-lb test (No. 295) was conducted as part of the PYRO program with conditions properly scaled to match these conditions



(weights scaled by factor of 1,000, times scaled by factor of 10). The measured combined yield for this test was 70%, which compares well with the predicted yield of 84%.

Section 6  
HEAT TRANSFER HAZARD

The fireball generated by the explosion of propellant mixtures can constitute a hazard primarily through heat transfer to an object or structure immersed in it.\* This section contains a description of the expected dimensions and duration of the associated fireball and of the heat flux density with time within it, each as a function of the quantity of propellants involved. Remarks indicating the basis and limitations of each prediction are also included.

The dimensions of the fireball depend generally on the quantity of propellants. An empirically derived expression relating the fireball dimension in terms of an equivalent diameter  $D$  in feet to the total propellant (fuel and oxidant) weight  $W$  in pounds for the propellant combinations of  $LO_2/RP-1$ ,  $LO_2/LH_2$ ,  $RP-1/LH_2/LO_2$ , and  $N_2O_4/50\% N_2H_4 - 50\% UDMH$  is given by\*\*

$$D = 9.56 W^{0.325} \quad (6.1)$$

where the estimated standard error in the diameter is 30%. Equation (6.1) does not always provide an accurate indication of the maximum dimension(s) of the fireball, since "in those instances where the fireballs were markedly asymmetrical, attempts were made to estimate equivalent spherical diameters."\*\*\* An indication of the departure from the diameter given in Eq. (6.1) of the maximum dimensions that can occur is provided, for instance, by the Titan test, which involved approximately 100,000 lb of  $LO_2/RP-1$ . The maximum horizontal fireball

---

\* Information permitting the evaluation of thermal hazards external to the fireball through radiant energy transfer are given in Section 6, Volume 1.

\*\* Equation (6.1), along with Eq. (6.2) below, have been extracted from J. B. Gayle and J. W. Bransford, Size and Duration of Fireballs from Propellant Explosions, NASA TM X-5312, August, 1965.

\*\*\* Ibid.

dimension from this test was estimated to be from 800 to 1000 ft, while Eq (6.1) indicates diameters of approximately 400 ft.

The fireball duration  $\tau$  in seconds, that is, the time over which fireball temperatures persist at hazardous levels (excluding residual fires of unburned propellants, which tend to collect in ground surface depressions or structural confinements) is given by,

$$\tau = 0.196 W^{0.349} \quad (6.2)$$

where the standard error in the duration is 84%.

Curves from which the heat flux density with time within the fireball can be obtained for a given propellant weight are given on Figs. 6-1 and 6-2 for the  $\text{LO}_2/\text{RP-1}$  and  $\text{LO}_2/\text{LH}_2$  propellant combinations, respectively. The time  $\tau_o$  in these figures is given in seconds by,

$$\tau_o = C W^{1/3} \quad (6.3)$$

for a total propellant weight  $W$  in pounds, with a value of  $C$  of 0.113 for  $\text{LO}_2/\text{RP-1}$  (Fig. 6-1) and of 0.077 for  $\text{LO}_2/\text{LH}_2$  (Fig. 6-2). Two curves are presented in each figure. One is the "bounding curve," which is an estimate of the upper bound of the heat flux density and is primarily based on the analysis of heat flux density data that were obtained from eleven 25,000-lb propellant tests, five of  $\text{LO}_2/\text{RP-1}$ , and six of  $\text{LO}_2/\text{LH}_2$ .<sup>\*</sup> The remaining curve, designated the "recommended curve," is superimposed on the bounding curve until a time  $\tau_o$  - given by Eq. (6.3) - where it abruptly decreases to zero. The recommended curves are also based primarily on analysis of the data from the eleven 25,000-lb tests

<sup>\*</sup> Data from which the heat flux density may be evaluated for the  $\text{N}_2\text{O}_4/50\% \text{N}_2\text{H}_4$  - 50% UDMH propellant combination are extremely limited. Examination of these data suggests that the heat flux density is somewhat less in magnitude than the bounding curves given for  $\text{LO}_2/\text{RP-1}$  and  $\text{LO}_2/\text{LH}_2$  in Figs. 6-1 and 6-2, but that the heating durations are perhaps somewhat larger.

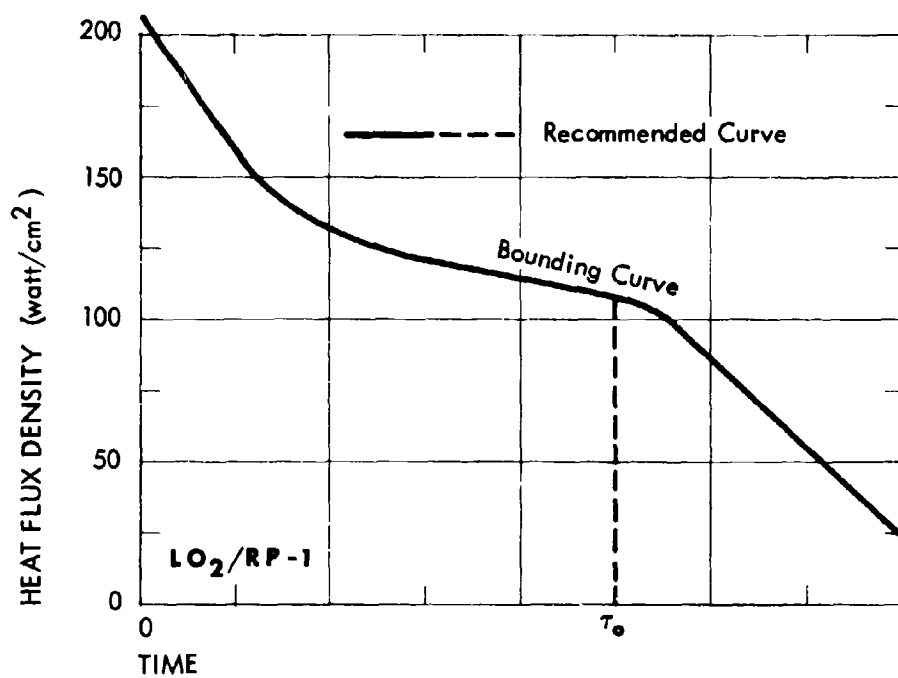


Fig. 6-1. Bounding and Recommended Heat Flux Density Curves

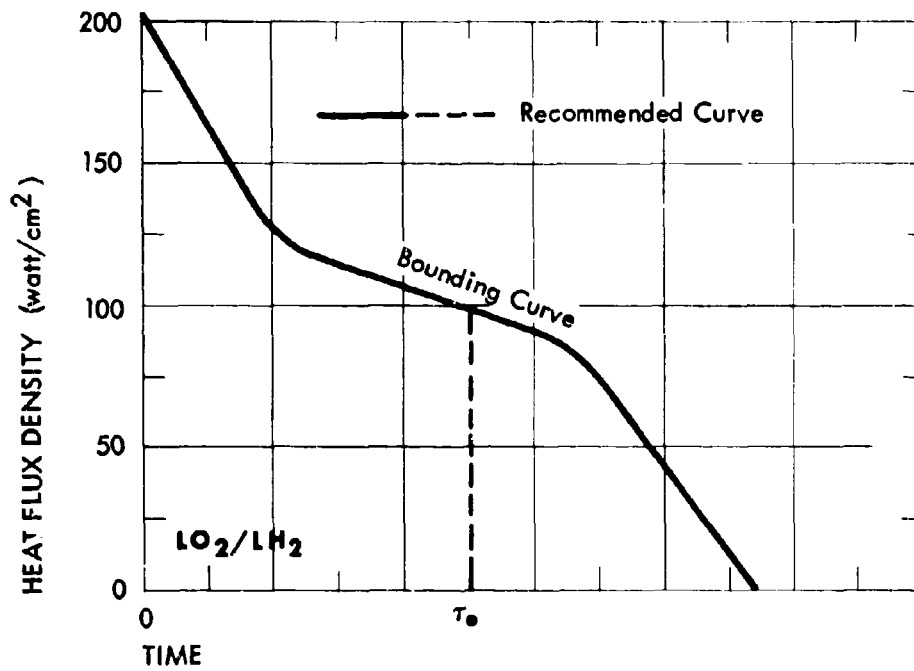


Fig. 6-2. Bounding and Recommended Heat Flux Density Curves

mentioned above, and implicitly contain the constraint that the probability of exceeding the cumulative heat flux density associated with the recommended curves (the time integration of the heat flux density from time equal zero to  $\tau_0$ ) is 1%. The variation of the heating pulse with propellant weight, that is, the scaling implicitly contained in Figs. 6-1 and 6-2 and Eq. (6.3), assumes, first, that the duration of the heating pulse will increase with the cube root of propellant weight, as implied by the empirical relation Eq. (6.2) and, second, that the heat flux density at a scaled time, using this cube root time scaling, will be invariant with variation in propellant weight. The second statement is based on the invariance of fireball temperatures (measured) from scale to scale.

No account has been made in the bounding or recommended curves for the emission of radiant energy from the surface of an immersed object, and this emission can substantially reduce the transfer rates from those given in the curves as the surface temperature of the object becomes a significant fraction of the fireball temperature, the latter being typically of the order of 2300°K. A reduction occurs similarly for the convective component of transfer. Any corresponding modifications of heat transfer from the curves, however, depend on the details of the application and are not considered here.

Several other qualifications of the bounding and recommended curves should be noted. First, the heat flux density measurements upon which the curves are primarily based were obtained from instruments that were fixed in space; thus, a modified heat flux density may be appropriate for objects which, for example, become prematurely ejected from the fireball (due, for instance, to blast wave forces). For many circumstances, the modification would be a reduction of the total heat transfer, first, due to the tendency to reduce the time that an object is immersed, and second, due to a reduction in the convective heat transfer component, since the motion imparted to the object by the blast wave forces would tend to reduce the relative velocity between the object and the surrounding gas. Rotary motion imparted to the object, however, would generally result in an increased transfer rate at given locations on the object. Whether it is appropriate to consider these factors in greater detail depends

again on the details of the particular application, and such factors are not discussed further here.

It can be seen from Eq. (6.3) that the heating durations of Figs. 6-1 and 6-2 (of either the bounding or recommended curves) increase with the cube root of propellant weight. This is an assumption that deserves some consideration. For comparatively small propellant quantities, say 1000 lb or less, the fireball duration is insufficient for appreciable motion (rise) of the fireball, and the fireball duration is then essentially synonymous with the heating duration of an object that is fixed in space. For larger propellant quantities, say for 25,000 lb and more, significant motion does occur and the heating duration of a fixed object is therefore less than the fireball duration. Thus, the ratio of the heating duration of a fixed object to the total fireball duration is some function of the propellant weight. The curves of Figs. 6-1 and 6-2 are based on measurements fixed in space at the 25,000-lb level, and extrapolation to other propellant weight levels through Eq. (6.3) inherently assumes an invariance of this ratio of durations. For application to weights in excess of 25,000 lb, it is nevertheless recommended that Eq. (6.3) be used in conjunction with the curves of Figs. 6-1 and 6-2, although it is expected that the curves would be somewhat conservative. For extrapolation to significantly lesser weights,  $\tau_o$  should be larger than given by Eq. (6.3); more specifically, at the 1000-lb (or less) level,  $\tau_o$  as given by Eq. (6.3) should be increased by a multiplying factor of approximately 1.2 and 1.6 for  $LO_2/ RP-1$  and  $LO_2/ LH_2$ , respectively.

It is possible that the heat transfer hazard can be intensified by the occurrence of chemical activity between the fireball constituents - notably the oxidants - and the surface of an object immersed in the fireball. Predictions of the rates (or existence) of the associated chemical reactions are not included in this report, in part due to the heavy dependence of such reactions on the particular application, that is, on the molecular constituents of the object and the surface temperature attained. The latter, in turn, depends on the configuration and thermal properties of the object. (The reaction also depends critically, of course, on the concentrations of various atomic and molecular

species - and their excited and ionized states - present in the fireball.) Chemical activity is mentioned and should be considered in any application - particularly when comparatively large propellant quantities are involved - because the reactions can provide an energy contribution (not included in Figs. 6-1 and 6-2) to the object.

The heat flux density measurements upon which the curves of Figs. 6-1 and 6-2 are based were obtained at locations no closer to the "center of explosion" than about one-fifth of the radius of the fireball, and it would be expected that the heat transfer rates, at least during the initial "small" fraction of the fireball duration, could be somewhat more severe at or "very near" the center of explosion. Passive sensors capable of providing crude indications of comparatively severe heat transfer were deployed in the central region (within a few feet of the planned ignition point) throughout most of the eleven 25,000-lb tests mentioned above, and a single positive indication was obtained. Specifically, from 0.1 to 0.2 in. was ablated from the surface of a solid aluminum structure in such a way as to suggest comparatively large heat flux densities over limited times, for instance, of the order of  $1000 \text{ watt/cm}^2$  for 2 sec. (A thorough analytic evaluation of the possible ranges of heat transfer parameters resulting in the above ablation has not been performed; for details of the aluminum structure and its ablation, see Appendix C of Volume 1.) It is not clear if chemical activity, as mentioned in the previous paragraph, was an energy contributor.



## Appendix A

## LIQUID PROPELLANT EXPLOSION PHENOMENA IN RELATION TO TNT

The characteristics of blast waves produced by explosive energy releases in air are in general dependent on three major groups of properties: those having to do with the intrinsic characteristics of the explosive material (explosive properties); those having to do with the manner in which the explosive material is assembled (charge properties); and those having to do with the environment surrounding the charge (environmental properties).

Explosive properties would include, for example, those necessary to describe the total energy release per gram of material (that contributes to the explosion) and the rate of energy release.

Charge properties would include those necessary to describe the total quantity of material, its shape, and any confinement effects due to inert material immediately adjacent to the charge.

Environmental properties, for example, would include those necessary to describe the nature of any ground surface in the vicinity of the charge, the location of the charge with respect to the ground surface (height of burst), and the ambient air pressure.

The explosive properties for most conventional solid high-explosive materials are quite similar and for a given material are often adequately described by simply stating the type of explosive. For liquid propellants, however, the range of explosive properties and thus the explosive behavior for a given propellant combination is extremely wide and generally differs considerably from that for conventional high explosives.

Specifically, for liquid propellant explosions the explosive yield or fraction of the total energy of the propellant mixture contributing to the explosion is not only dependent on propellant type, but also on certain other parameters, including, for example,

1. propellant interaction geometry (mixing mode)
2. time of ignition
3. various initial conditions, such as spatial and velocity distribution of propellants at time of contact
4. propellant weight

In addition, the shapes of the propellant pressure-distance and impulse-distance curves are not necessarily identical to those for TNT.

To summarize, the parameters which generally control the important blast characteristics of liquid propellant explosions, i.e., peak overpressure and positive-phase impulse, are: \*

- |   |   |
|---|---|
| 1. total propellant weight                            | W |
| 2. fraction of total energy contributing to explosion | f |
| 3. nature of reaction                                 | m |
| 4. ground distance                                    | D |
| 5. height of burst                                    | h |
| 6. charge shape                                       | s |

By means of normal explosive scaling laws, the parameter list can be reduced to:

- |                           |                |
|---------------------------|----------------|
| 1. nature of reaction     | m              |
| 2. scaled ground distance | $D/(fW)^{1/3}$ |
| 3. scaled height of burst | $h/(fW)^{1/3}$ |
| 4. charge shape           | s              |

For some conditions it is possible that f may be a function of W.

---

\* Confinement effects, ambient overpressure, and nature of ground surface may have to be considered in special circumstances, but in most applications they do not vary sufficiently to require consideration.

Considering for the moment a surface burst condition\* and a constant charge shape, only two basic parameters are left:

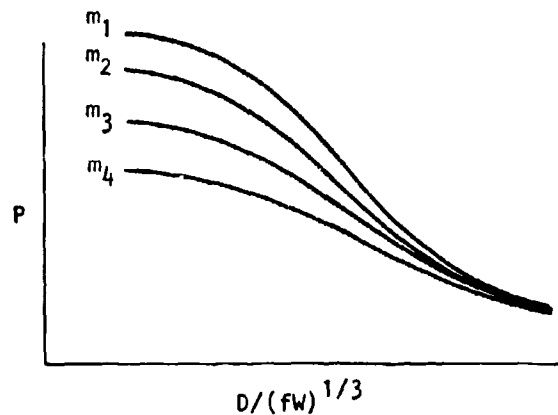
1. nature of mixture

$m$

2. scaled ground distance

$D/(fw)^{1/3}$

Conceptually, therefore, all desired data on overpressure (or impulse) for a given propellant combination (under surface burst conditions and with a constant charge shape), could be expressed in a single plot as follows:



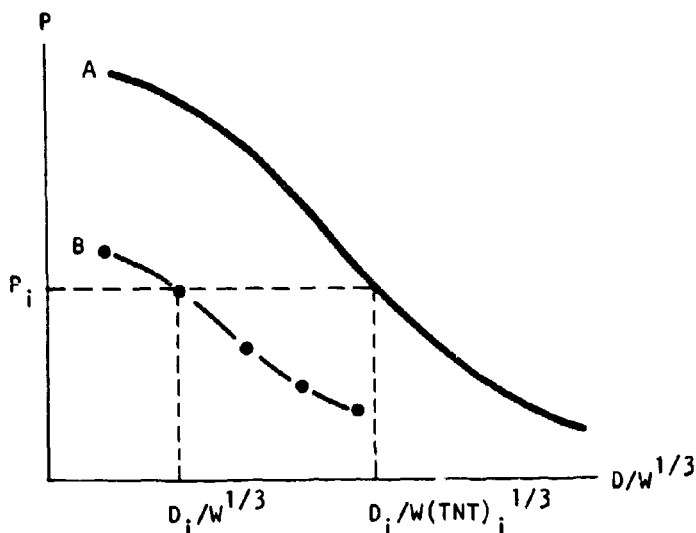
At this stage it is appropriate to consider in more detail what the factors  $f$  and  $m$  mean. Earlier  $f$  was defined as the fraction of the total energy contributing to the explosion. This actually is a somewhat loose definition. It could be argued, for example, that  $f$  is generally not the effective fraction of energy released to produce a given overpressure or impulse value since this also depends on  $m$ , as illustrated in the above figure. Rather,  $f$  is intended as a measure of the total amount of energy released in the explosion that ultimately contributes to the blast wave, while  $m$  is intended as a measure of the manner or rate of energy release. The reason for separating the factors  $f$  and  $m$ ,

\* Considered in this report to be a hemispherical charge on the surface.

rather than attempting to use them in some combined fashion, is that, first, they depend on somewhat different sets of basic parameters and, secondly, there is generally a significant range of distances of interest (at intermediate to long distances from the explosion) where the  $m$  values become unimportant and the  $f$  value alone controls the overpressure and impulse values. Also, in this region the  $f$  values for both overpressure and impulse are the same.\*

Within the definition of the  $f$  and  $m$  factors given above there is still some choice of how to quantitatively determine them from experimental data and to use them in a prediction method. The method used in this report for determining the  $f$  factor is based on TNT equivalence and is described below.

Assume, for example, in the figure below that curve A is the "standard" TNT surface burst overpressure-distance curve and curve B is the curve for a particular test condition involving  $W_p$  lb of propellant (curve B points are plotted using  $W_p$  for computing scaled distance values).



\* This occurs because as a blast wave proceeds into the ambient air surrounding its source, its behavior tends to be controlled by the ambient air it is propagating through, and the influence of the specific nature of the source becomes progressively less important with increasing distance from the source.

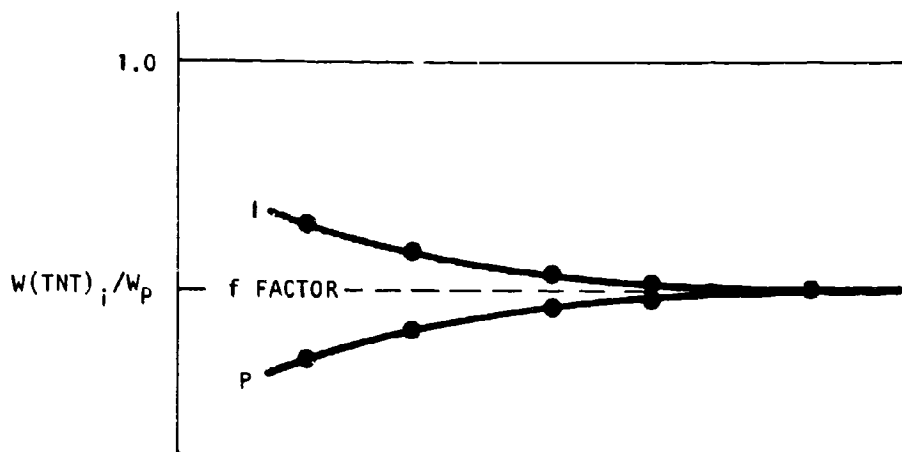
For each experimental point on curve B ( $P_1$ ,  $D_1$ ) the weight of TNT,  $W(TNT)_1$ , necessary to produce the same overpressure at the distance  $D_1$  as obtained in the particular test is computed by:

1. determining the value of the scaled distance ( $D_1/W(TNT)_1^{1/3}$ ) from curve A for the overpressure  $P_1$
2. dividing  $D_1$  by this scaled distance and cubing the results, i.e.,

$$W(TNT)_1 = \left[ \frac{D_1}{D_1/W(TNT)_1^{1/3}} \right]^3$$

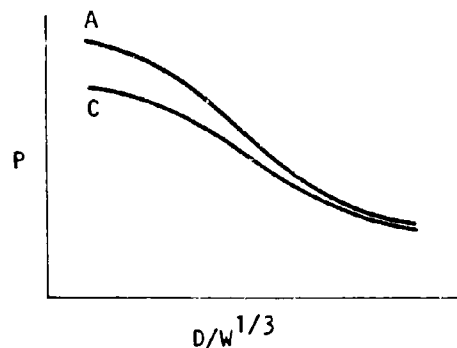
A similar process would be carried out for the impulse data.

The ratios of  $W(TNT)_1/W_p$  are then plotted as a function of distance as shown below:



The f factor is then the particular value of the ratio of  $W(TNT)_1/W_p$  approached by both the overpressure and impulse data at long distances. Thus the f factor is simply the terminal explosive yield.

By means of the  $f$  factor so determined, the experimental data points can be replotted using  $fw_p$  for computing scaled distance and compared with the ideal curve A as shown below. (C is curve B so replotted.)



The remaining differences between curves A and C : due to the  $m$  factor.

The PYRO data clearly show the general trends discussed above. The differences between the propellant and TNT overpressure-distance and impulse-distance curves were largest for the hypergolic combination, and both pressure and impulse correction factors were derived as a function of scaled distance. For the cryogenic propellants the effects were somewhat smaller, and it was only possible to derive impulse correction factors. The propellant pressure data tended to be below the TNT curve, but the spread was large enough so that the TNT curve was used as a conservative bound. It should be emphasized that such a bound is believed to be overly conservative for distances closer than about 2 scaled feet ( $\text{ft/lb}^{1/3}$ ). Unfortunately insufficient data were obtained in this region to actually define the curve.

URS 652-35

AFRPL-TR-68-92

Appendix B

PEAK OVERPRESSURE VS DISTANCE AND POSITIVE-PHASE IMPULSE  
VS DISTANCE REFERENCE CURVES

